Materials Letters 418 (2026) 140880

Contents lists available at ScienceDirect

Materials Letters

journal homepage: www.elsevier.com/locate/matlet

Micro-tensile testing for strength characterization of high-speed steel

Leonhard Gertlowski [a,b,*], Tobias Sedlatschek [a,b], Oliver Schenk [a], Stefan Müller [c], Santiago Benito [c], Sebastian Weber [c], Christoph Broeckmann [a,b]

[a] Institute for Materials Applications in Mechanical Engineering (RWTH Aachen University), Augustinerbach 4, Aachen 52062, Germany
[b] Institute of Applied Powder Metallurgy and Ceramics at RWTH Aachen e.V., Augustinerbach 4, Aachen 52062, Germany
[c] Chair of Materials Technology (Ruhr University Bochum), Universitätsstraße 150, Bochum 44801, Germany

ARTICLE INFO

Keywords:
Micro-tensile test
Push-to-pull
Focused ion beam
Interfacial strength
High-speed steel

ABSTRACT

The high-speed steel PM HS3–3–4 was investigated to assess the influence of an isothermal holding stage within the transformation gap during quenching on the interfacial strength between the matrix and carbides. The interfacial strength was assessed by micro-tensile testing using push-to-pull geometries fabricated via focused ion beam (FIB) milling. During indentation, the gauge section was continuously recorded by scanning electron microscopy (SEM) and strain analysis was conducted by digital image correlation (DIC). Tensile strengths of 2150–2500 MPa, unaffected by the isothermal holding stage, were measured together with significant plastic deformation in the martensitic matrix. Fracture occurred within the matrix in close proximity to the interface.

1. Introduction

High-speed steels (HSS), a subclass of tool steels, are iron-based alloys containing carbon, chromium, vanadium, tungsten and/or molybdenum, with optional additions of cobalt. They combine high hot hardness, wear resistance, and fracture toughness, which are essential for cutting tool applications operating at service temperatures up to 600 °C [1]. The pronounced hot hardness in HSS arises from carbide precipitation induced by multiple tempering cycles, whereas wear resistance is predominantly governed by the larger eutectic carbides [2,3]. In contrast to ingot-cast HSS, powder metallurgical (PM) HSS exhibit carbides embedded in the martensitic matrix that are more uniformly distributed, predominantly spherical and typically a few micrometers in size [1]. The carbide-matrix interfaces are incoherent [4]. A strong interfacial bonding between these larger carbides and the martensitic matrix is crucial for preventing carbide detachment or subsurface damage under abrasive wear conditions, thereby enhancing tool life [5].

An isothermal holding stage within the transformation gap during quenching of HSS promotes the formation of rounder carbides [6]. It is hypothesized that the carbides grow epitaxially from the surrounding matrix. The isothermal holding stage further enhances the amount of martensite formed during the subsequent cooling to room temperature [7]. However, the influence of this isothermal holding stage and the associated epitaxial carbide growth on the interfacial bonding strength between carbide and matrix has not yet been investigated. In the present study, micro-tensile testing was employed for the first time to directly characterize the carbide-matrix interface in HSS, i.e., to quantify its interfacial bonding strength and to assess the potential of an isothermal holding stage for improving abrasive wear resistance. A push-to-pull geometry optimized for a uniaxial and homogeneous stress state was employed [8].

2. Materials and methods

In this study, gas-atomized PM HS3–3–4 (DIN EN 1.3377) powder with a particle size below 500 µm (D_{50} = 159 µm) and the chemical composition given in Table 1 was employed. The powder was processed by the PM route, employing hot isostatic pressing (HIP) as consolidation technique. For this purpose, the powder was filled into cylindrical capsules made of stainless steel (DIN EN 1.4541). The capsules were evacuated for 24 h, sealed and subsequently heated to 1100 °C. HIP was performed in a Quintus type URQ-HIP furnace at a pressure of 150 MPa for 4 h. Both capsules were cooled down under pressure in the HIP unit, one was quenched directly to room temperature, whereas the other was cooled to 520 °C, held for 1 h at 150 MPa within the transformation gap, and then quenched to room temperature. Both capsules were subsequently tempered three times at ambient pressure at 560 °C for 1 h each.

The heat treated HSS was characterized by micro-tensile testing. The interfacial strength between the matrix and carbides was evaluated

* Corresponding author at: Institute for Materials Applications in Mechanical Engineering (RWTH Aachen University), Augustinerbach 4, Aachen 52062, Germany.
E-mail address: l.gertlowski@iwm.rwth-aachen.de (L. Gertlowski).

https://doi.org/10.1016/j.matlet.2026.140880
Received 17 March 2026; Received in revised form 1 May 2026; Accepted 10 May 2026
Available online 11 May 2026
0167-577X/© 2026 The Authors. Published by Elsevier B.V. This is an open access article under the CC BY license (http://creativecommons.org/licenses/by/4.0/).

Table 1
Chemical composition of PM HS3–3–4 powder determined by optical emission spectroscopy and combustion analysis. All values are given in wt% except for O (ppm).

C	Si	Mn	P	S	Co	Cr	Mo	V	W	N	Fe	O
1.453 ± 0.100	0.472 ± 0.013	0.274 ± 0.004	0.043 ± 0.003	0.032 ± 0.003	0.629 ± 0.008	4.19 ± 0.04	2.48 ± 0.07	4.12 ± 0.05	2.75 ± 0.08	0.031 ± 0.003	Bal.	113 ±7

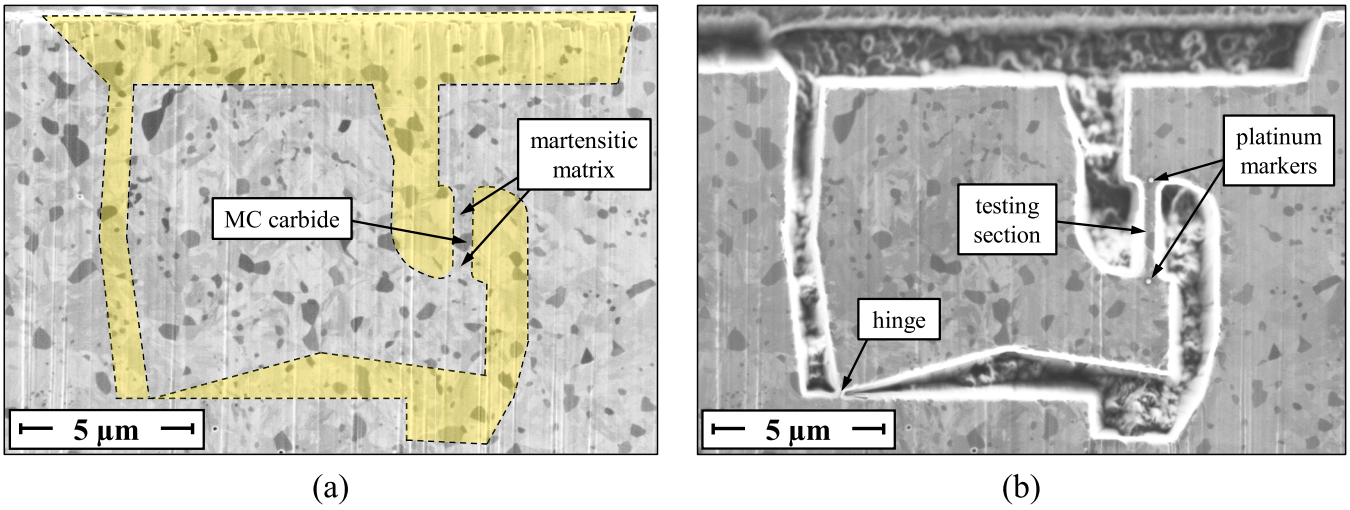


Fig. 1. Microstructure of PM HS3–3–4 with regions to be removed via FIB milling (a) and the hereby produced push-to-pull test geometry (b).

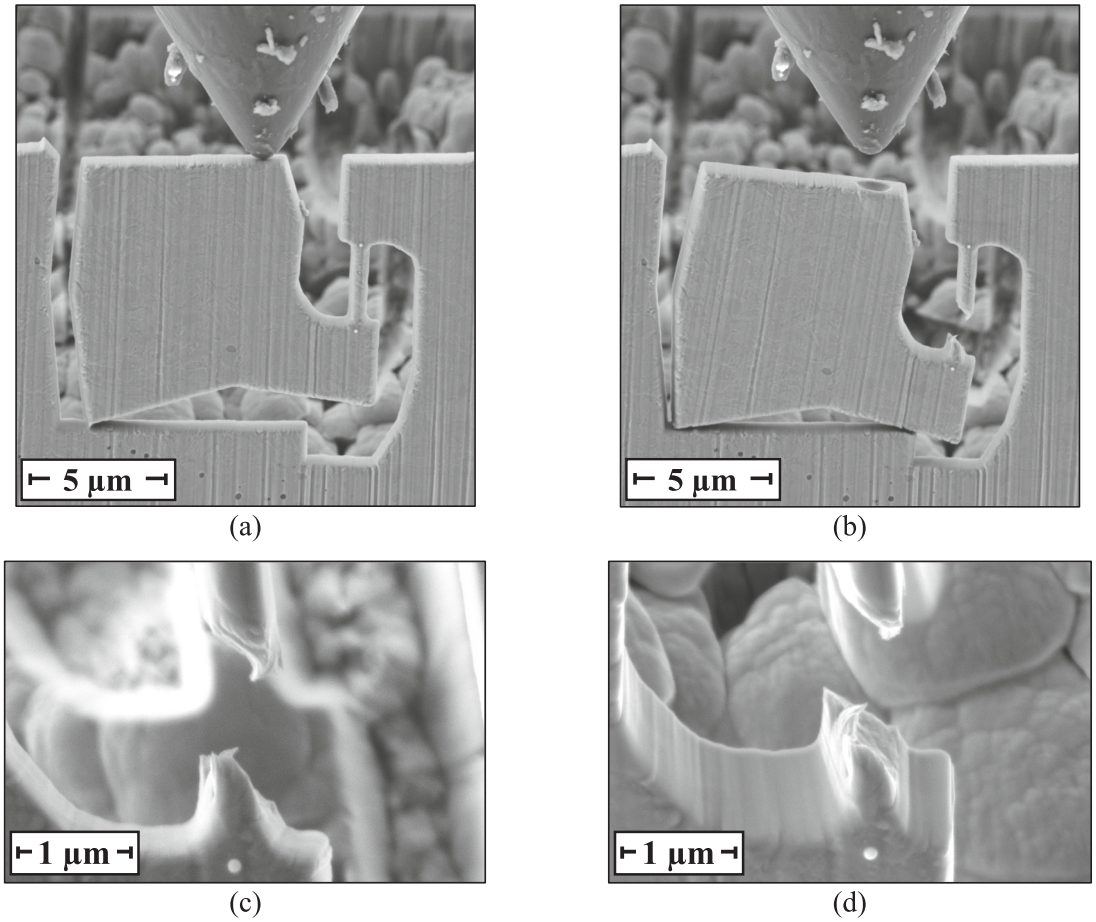


Fig. 2. Push-to-pull geometry before (a) and after (b) micro-tensile testing, with the fracture surface shown at different tilt angles (c, d).

employing a push-to-pull geometry (Fig. 1), which was fabricated by FIB milling in a *FEI Helios NanoLab G3 CX Dual-Beam FIB-SEM*. This

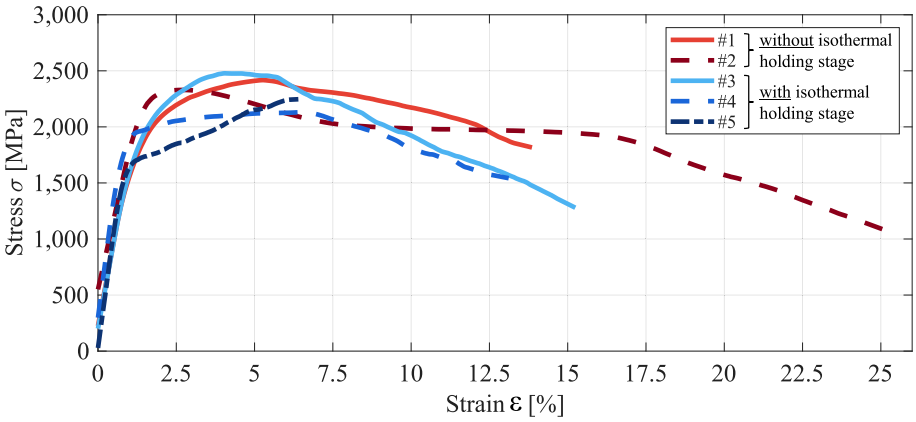


Fig. 3. Engineering stress-strain curves of PM HS3–3–4 from micro-tensile testing, comparing specimens quenched with and without an isothermal holding stage in the transformation gap.

geometry was previously optimized in [8] to ensure a homogeneous and uniaxial stress state within the testing section by eliminating bending moments through deformations of the region below and above the gauge section. During indentation, the testing section was continuously recorded by a *Tescan CLARA SEM* at a frame rate of 3 fps. Post-mortem strain analysis was performed via DIC using platinum markers being deposited before testing by a gas-injection-system (GIS) at both ends of the gauge section of 3 µm in length. A carbide-containing testing section with two carbide-matrix interfaces was fabricated by FIB milling. The gauge cross-section dimensions were approximately 0.6 µm × 1.4 µm. The resulting stress-strain curves were subsequently compared for PM HS3–3–4 samples processed with and without the isothermal holding stage in the transformation gap during quenching.

Micro-tensile testing was carried out with a *Bruker Hysitron PI 89 SEM PicoIndenter* equipped with a *Synton-MDP* diamond spherical tip (tip radius 1 µm), as shown in Fig. 2. A small material ligament connecting the micro-tensile geometry to the surrounding material acts as a hinge. As reported in [8], the stiffness of this hinge is negligible. Taking into account the lever geometry, the indenter was actuated at a displacement rate of 0.5 $nm \cdot s^{-1}$ to obtain a nominal strain rate of $2.5 \cdot 10^{-4}\ s^{-1}$ in the gauge section, consistent with DIN EN ISO 6892-1 for macroscopic tensile testing.

3. Results and discussion

In this study, micro-tensile testing was performed on PM HS3–3–4, consolidated by PM-HIP, with and without an isothermal holding stage in the transformation gap during quenching. The results, post-processed using a *Savitzky-Golay* filter, are shown in Fig. 3. Although HSS typically exhibit low fracture strains in macroscopic tensile tests [9], significantly higher total fracture strains - ranging from 7% to 25% - and a ductile fracture surface (Fig. 2(d)) were observed in micro-tensile testing. Before interface decohesion, plastic deformation is observed on the metallic side of the interface. This observation is consistent with studies on the interface of TiN-coated HSS, in which the TiN was sheared relative to the martensitic matrix under combined shear-compressive loading [10]. The extremely small gauge cross-section increases the likelihood that the tested volume exhibits a uniform martensitic lath orientation. In contrast to macroscopic specimens, which exhibit local multiaxial stress states owing to the random orientation of anisotropic martensitic laths, strain incompatibilities between neighboring grains are significantly reduced in the micro-scale geometry. The reduced stress triaxiality results in a more ductile response of the micro-tensile specimens. Moreover, the micro-tensile specimens exhibit a slenderness ratio $\sqrt{A}/L$ nearly twice that of the macroscopic specimens specified in DIN EN ISO 6892-1, where A denotes the cross-sectional area and L the gauge length. The larger slenderness ratio is consistent with a higher fracture strain [11]. The scatter in fracture strain can be attributed to variations in the orientation of the martensitic lath structure among the individual micro-tensile specimens and to small notches as artifacts from FIB milling.

The reliability of the experimental setup was evaluated by estimating the Young's modulus from the linear-elastic region of the engineering stress-strain curves. The mean value of 245 GPa (with a standard deviation of 30 GPa) shows good agreement with macroscopic testing results for PM HS3–3–4, thereby supporting the plausibility of the micro-tensile tests.

The tensile strength ranges from 2150 to 2500 MPa. No significant difference was observed between the micro-tensile specimens with and without an isothermal holding stage in the transformation gap during quenching. All specimens fractured in close proximity to the carbide-matrix interface, with material separation occurring within the matrix. This raises the question of why no brittle fracture along the interface was observed. Under uniaxial loading, increasing tensile stress leads to lateral contraction of the gauge section. Since carbides exhibit a higher Young's modulus and a lower Poisson's ratio than the martensitic matrix [12], the resulting constraint leads to a multiaxial stress state close to the interface in the matrix, ultimately leading to failure within the martensitic matrix rather than at the interface. It can thus be concluded that the interfacial strength of the carbides exceeds the cohesive strength of the martensitic matrix.

The results indicate that the isothermal holding stage in the transformation gap during quenching does not affect the strength of the martensitic matrix surrounding the interface. Accordingly, the potential of the isothermal holding stage to enhance the wear resistance of HSS cutting tools under abrasive wear conditions could not be substantiated in this study. Further experiments under real wear conditions at the tool-workpiece contact are required to assess the effect of the isothermal holding stage on wear resistance.

4. Conclusion

In this study, micro-tensile testing was performed on HSS for the first time for this material. The push-to-pull geometry, optimized for uniaxial loading, was tested using a spherical indenter while recording the deformation up to fracture. Stress-strain curves were derived from DIC analysis. Significantly higher fracture strains compared to macroscopic tensile tests were observed. The increased fracture strain is attributed, among other factors, to a more uniform orientation of the martensitic lath structure. The cohesive strength of the martensitic matrix of the heat-treated PM HS3–3–4 ranges between 2150 and 2500 MPa, with no significant difference between specimens tested with and without an isothermal holding stage in the transformation gap during quenching. However, under the loading conditions of this study, failure occurs

preferentially in the matrix, indicating that the interface is not the weakest link. The fracture within the matrix is attributed to the multi-axial stress state caused by the mismatch in lateral contraction between matrix and carbide.

CRediT authorship contribution statement

Leonhard Gertlowski: Writing – review & editing, Writing – original draft, Visualization, Methodology, Investigation, Data curation, Conceptualization. **Tobias Sedlatschek:** Writing – review & editing, Writing – original draft, Methodology, Investigation, Conceptualization. **Oliver Schenk:** Writing – review & editing, Writing – original draft, Supervision, Conceptualization. **Stefan Müller:** Writing – review & editing. **Santiago Benito:** Writing – review & editing, Supervision. **Sebastian Weber:** Writing – review & editing, Supervision, Resources, Funding acquisition. **Christoph Broeckmann:** Writing – review & editing, Supervision, Resources, Funding acquisition.

Declaration of competing interest

The authors declare that they have no known competing financial interests or personal relationships that could have appeared to influence the work reported in this paper.

Acknowledgments

We acknowledge the funding of the project “Influence of Integrated HIP Heat Treatments on the Microstructure and Mechanical Properties of a PM Tool Steel: Experiment and Simulation” from the German Research Foundation (Grant number: 532214230).

Data availability

Data will be made available on request.

References

[1] J. Schlegel, Schnellarbeitsstahl: Ein Stahlporträt, Springer Vieweg, Wiesbaden, 2022.
[2] F. Bergman, P. Hedenqvist, S. Hogmark, The influence of primary carbides and test parameters on abrasive and erosive wear of selected PM high speed steels, Tribol. Int. 30 (1997) 183–191, https://doi.org/10.1016/S0301-679X(96)00040-0.
[3] N. Wulbieter, F. Pöhl, W. Theisen, Influence of hot hardness and microstructure of high-alloyed powder metallurgical tool steels on abrasive wear behavior at elevated temperatures, Steel Res. Int. 91 (2020) 1900461, https://doi.org/10.1002/srin.201900461.
[4] E. Pippel, J. Woltersdorf, G. Pöckl, G. Lichtenegger, Microstructure and nanochemistry of carbide precipitates in high-speed steel S 6-5-2-5, Mater. Charact. 43 (1999) 41–55, https://doi.org/10.1016/S1044-5803(99)00003-0.
[5] G.Y. Lee, C. Dharan, R. Ritchie, A physically-based abrasive wear model for composite materials, Wear 252 (2002) 322–331, https://doi.org/10.1016/S0043-1648(01)00896-1.
[6] N. Disch, S. Benito, A. Röttger, S. Weber, Influence of heat treatment parameters on the carbide morphology of PM high-speed steel HS 6-5-3-8, Steel Res. Int. 94 (2023) 2200755, https://doi.org/10.1002/srin.202200755.
[7] J. Kaleicheva, V. Mishev, Bainitic transformation in high-speed steels, Teh. Vjesn. 26 (2019), https://doi.org/10.17559/TV-20180327165425.
[8] T. Sedlatschek, L. Gertlowski, F. Weber, C. Broeckmann, Characterization of the grain boundary strength of polycrystalline NMC811 using in situ micro tensile tests, Preprint (2026), https://doi.org/10.2139/ssrn.6429437.
[9] P. Brøndsted, P. Skov-Hansen, Fatigue properties of high-strength materials used in cold-forging tools 1, Int. J. Fatigue 20 (1998) 373–381, https://doi.org/10.1016/S0142-1123(98)00006-1.
[10] M. Gsellmann, T. Klünsner, C. Mitterer, M. Krobath, M. Wurmshuber, H. Leitner, W. Ecker, S. Marsoner, V. Maier-Kiener, D. Kiener, G. Ressel, Strength ranking for interfaces between a TiN hard coating and microstructural constituents of high speed steel determined by micromechanical testing, Mater. Des. 204 (2021) 109690, https://doi.org/10.1016/j.matdes.2021.109690.
[11] L. Li, J.W. Merickel, Y. Tang, R. Song, J.E. Rittenhouse, A. Vakanski, F. Xu, Empirical validation of size effects in sub-sized tensile specimens for nuclear structural materials, Sci. Rep. 15 (2025) 13846, https://doi.org/10.1038/s41598-025-98849-5.
[12] H.O. Pierson, Handbook of Refractory Carbides and Nitrides: Properties, Characteristics, Processing, and Applications, Noyes Publications, Westwood, NJ, 1996.